ORIGINAL ARTICLE

Communication between human macrophages and epithelial cancer cell lines dictates lipid mediator biosynthesis

Markus Werner[1] · Simona Pace[1] · Anna Czapka[1] · Paul M. Jordan[1] · Jana Gerstmeier[1] · Andreas Koeberle[1,2] · Oliver Werz[1]

Abstract

In tumors, cancer cells coexist and communicate with macrophages that can promote tumorigenesis via pro-inflammatory signals. Lipid mediators (LMs), produced mainly by cyclooxygenases (COXs) or lipoxygenases (LOs), display a variety of biological functions with advantageous or deleterious consequences for tumors. Here, we investigated how the communication between human monocyte-derived M2-like macrophages (MDM) and cancer cells affects LM biosynthesis using LM metabololipidomics. Coculture of human MDM with human A549 epithelial lung carcinoma cells, separated by a semipermeable membrane, increased LM formation by MDM upon subsequent activation. Strongest effects were observed on 5-LO-derived LM. While expression of the 5-LO pathway was not altered, p38 MAPK and the downstream MAPKAPK-2 that phosphorylates and stimulates 5-LO were more susceptible for activation in MDM upon precedent coculture with A549 cells as compared to monocultures. Accordingly, the p38 MAPK inhibitor Skepinone-L selectively prevented this increase in 5-LO product formation. Also, 5-LO-/15-LO-derived LM including lipoxin A_4, resolvin D2 and D5 were elevated after coculture with A549 cells, correlating to increased 15-LO-1 protein levels. In contrast to cancer cells, coincubation with non-transformed human umbilical vein endothelial cells (HUVEC) did not affect LM production in MDM. Vice versa, MDM increased COX-2 protein expression and COX-mediated prostanoid formation in cancer cells. Conclusively, our data reveal that the communication between MDM and cancer cells can strikingly modulate the biosynthetic capacities to produce bioactive LM with potential relevance for tumor biology.

Abbreviations

AA	Arachidonic acid
COX	Cyclooxygenase
$cPLA_2$-α	Cytosolic phospholipase A_2-α
DHA	Docosahexaenoic acid
EPA	Eicosapentaenoic acid
ERK-1/2	Extracellular signal-regulated protein kinase-1/2
FCS	Fetal calf serum
FLAP	5-Lipoxygenase-activating protein
HETE	Hydroxyeicosatetraenoic acid
HUVEC	Human umbilical vein endothelial cells
LM	Lipid mediator
LO	Lipoxygenase
LT	Leukotriene
MAPK	Mitogen-activated protein kinase
MK-2	MAPKAPK-2, mitogen-activated protein kinase-activated protein kinase-2
MDM	Monocyte-derived macrophages
NSAID	Non-steroidal anti-inflammatory drugs
PG	Prostaglandin
SPM	Specialized pro-resolving mediators
TAM	Tumor-associated macrophages

Markus Werner and Simona Pace contributed equally.

Electronic supplementary material The online version of this article (https://doi.org/10.1007/s00018-019-03413-w) contains supplementary material, which is available to authorized users.

✉ Simona Pace
simona.pace@uni-jena.de

✉ Oliver Werz
oliver.werz@uni-jena.de

[1] Department of Pharmaceutical/Medicinal Chemistry, Institute of Pharmacy, Friedrich-Schiller-University, Philosophenweg 14, 07743 Jena, Germany

[2] Michael Popp Research Institute, University of Innsbruck, Mitterweg 24, 6020 Innsbruck, Germany

| TME | Tumor microenvironment |
| UPLC-MS–MS | Ultra performance liquid chromatography-tandem mass spectrometry |

Introduction

Tumors are composed of different cell types that are exposed to a variety of bioactive mediators, which together form the tumor microenvironment (TME) [1]. Besides cancer cells, endothelial cells, and fibroblasts, also immune cells, particularly tumor-associated macrophages (TAM), occur in tumors [2–4]. Macrophages can accumulate in tumors by proliferation from precursors that are resident in tissues or by trafficking from bone-marrow undergoing differentiation towards mature macrophages [2, 4]. Once in tumors, these recruited macrophages can adopt a tumor-supporting subtype secreting cytokines, chemokines and other bioactive mediators that induce immunosuppression, angiogenesis, tumor growth, and metastasis [2]. Macrophages can adopt a wide spectrum of phenotypes where simplified extremes can be divided into "anti-tumoral" M1 and "pro-tumoral" M2 [5]. TAM usually display a M2-like phenotype, and higher M2-like TAM infiltration correlates with poor prognosis [3, 6].

Lipid mediators (LM) comprise different classes of bioactive lipids that act as local hormones mediating their multiple actions via cognate G-protein-coupled receptors [7]. The majority of LM that are derived from polyunsaturated fatty acids are generated by stereospecific oxygenation via cyclooxygenase (COX) and lipoxygenase (LO) pathways and play crucial roles in acute and chronic inflammation [8]. While COX-1/2 convert arachidonic acid (AA; 20:4 ω-6) to initialize the biosynthesis of pro-inflammatory prostanoids, particularly prostaglandin (PG)E_2, the 5-LO pathway leads to formation of leukotrienes (LT) from AA that possess inflammatory properties, too [9]. In contrast, the novel superfamily of so-called specialized pro-resolving mediators (SPM) are generated from docosahexaenoic acid (DHA) and eicosapentaenoic acid (EPA), mainly involving 12-/15-LOs that act in conjunction with 5-LO, and possess anti-inflammatory features by actively terminating inflammatory responses and by promoting the resolution of inflammation [10, 11].

Unresolved inflammation is a well-recognized hallmark of cancer, and chronic inflammatory diseases can increase the risk for cancers [12, 13], while drugs interfering with inflammation, e.g., non-steroidal anti-inflammatory drugs (NSAIDs), are chemopreventive [14, 15]. NSAIDs mediate their anti-inflammatory effects by inhibiting COX-mediated prostanoid formation, and along these lines, PG as well as LT orchestrate the complex interactions between cancer cells and the surrounding stromal cells in tumors in relation to tumor progression and metastasis [16, 17]. 5-LO and COX-2 are known to be overexpressed in several cancers including lung, colon, breast, prostate, and pancreas, and LT and PG are commonly elevated in tumors with obvious roles in tumorigenesis and metastasis [17–19]. Indeed, cancer patients with increased COX-2 levels in their tumors exhibit decreased survival rates [17, 18], and genetic or pharmacological inhibition of 5-LO in neutrophils abrogated lung colonization of metastasis-initiating breast cancer [20]. In contrast, SPM suppress tumor growth [21] and stimulate resolution in cancer by enhancing endogenous clearance of tumor cell debris [22].

The cancer lipidome is rather diverse and may obviously promote but also inhibit cancer pathogenesis [15]. In the tumor, cancer cells and TAM as well as other stromal cells coexist and communicate with each other, leading to specific alterations in the LM signature profiles compared to those of cells in healthy tissues [23, 24]. Tumor-specific LM profiles are caused on one hand by coordinated transcellular LM biosynthesis by the multiple cell types and enzymes involved [25] but also by aberrant expression of LM-biosynthetic enzymes due to cancer cell-stromal cell interactions within the TME [17]. Here, we designed a coculture system of cancer cells and human TAM-like monocyte-derived macrophages (MDM) without direct contacts between the cells to study how their humoral communication influences LM biosynthesis pathways in each cell type.

Materials and methods

Cells, cell isolation, and differentiation of monocyte-derived macrophages

The human acute promyelocytic leukemia cell line HL-60 (ATCC) was cultured in RPMI-1640 (GE Healthcare Life Sciences, South Logan, UT) supplemented with 10% (v/v) heat-inactivated fetal calf serum (FCS), 2 mmol/l (L-glutamine), penicillin (100 U/ml), and streptomycin (100 µg/ml) in a humidified atmosphere at 37 °C and 5% CO_2.

Human epithelial lung carcinoma A549 cells (ATCC) and human colon cancer HT-29 cells (ATCC) were cultured in DMEM (Biochrom/Merck, Berlin, Germany) supplemented with 10% (v/v) heat-inactivated FCS, penicillin (100 U/ml), and streptomycin (100 µg/ml) in a humidified atmosphere at 37 °C and 5% CO_2.

Human umbilical vein endothelial cells (HUVEC) were isolated from human umbilical cords and cultured in "Endothelial Cell Basal Medium MV" supplemented with "Endothelial Cell Growth Medium MV2 SupplementMix" (PromoCell, Heidelberg, Germany) for up to four passages as described previously [26]. Donors were informed about the aim of the study and gave written informed consent.

Monocytes were isolated from leukocyte concentrates derived from freshly withdrawn peripheral venous blood of healthy adult (18–65 years) human donors (Institute of Transfusion Medicine, University Hospital Jena, Germany). The experimental protocol was approved by the ethical committee of the University Hospital Jena, and all methods were performed in accordance with the relevant guidelines and regulations. Peripheral blood mononuclear cells (PBMC) were isolated using dextran sedimentation and Ficoll-Histopaque 1077-1 (Sigma-Aldrich, Taufkirchen, Germany) centrifugation. Monocytes were obtained from PBMC by adherence to cell culture flasks (Greiner Bio-One, Frickenhausen, Germany) for 1.5 h (37 °C, 5% CO_2) in phosphate-buffered saline (PBS) pH 7.4 supplemented with 1 mM Ca^{2+} and 0.5 mM Mg^{2+}, followed by removing non-adherent cells and adding fresh medium (RPMI 1640 containing 2 mM L-glutamine, 10% heat-inactivated FCS, 100 U/ml penicillin and 100 µg/ml streptomycin). For differentiation towards TAM-like macrophages, monocytes were first incubated with 20 ng/ml macrophage colony-stimulating factor (M-CSF; PeproTech, Hamburg, Germany) for 6 days, followed by so-called alternative activation using 20 ng/ml interleukin (IL)-4 (PeproTech) for additional 48 h [27].

Cocultures of cancer cells or HUVECs with MDM were performed in a Boyden chamber system composed of 6-well plates—advanced TC (Greiner Bio-One) as lower compartment, and Falcon Cell Culture inserts with 0.4 µm pore size (VWR International, Darmstadt, Germany) as upper compartment. Cancer cells or HUVECs were seeded in the lower compartment (2×10^6 cells in 2 ml medium). After 2 h, inserts were installed on top of the wells, immediately followed by addition of MDM (2×10^6 cells/ml) to the other compartment. Both compartments received RPMI-1640 containing 10% FCS, 2 mM L-glutamine, 100 U/ml penicillin, and 100 µg/ml streptomycin for cocultures with cancer cell lines or "Endothelial Cell Growth Medium" including "SupplementalMix" for HUVEC cocultures. After 2 h, IL-4 (20 ng/ml) was added to the Boyden chamber system with access to both compartments. Cells were cocultured (or monocultured in case of controls) for another 48 h. Then, cell populations were separated from each other for conducting further analysis.

Incubations of MDM, cancer cells or HUVEC and LM metabololipidomics

The different cell types from the Boyden chamber cocultures were separated from each other. MDM, cancer cells or HUVECs (2×10^6 cells) were incubated in 2 ml of PBS pH 7.4 containing 1 mM $CaCl_2$. For experiments using Skepinone-L (0.3 µM) the test compound or vehicle (0.1% DMSO) were applied 15 min prior stimulation. Cells were exposed to *E. coli* (serotype O6:K2:H1) at a ratio of 1:50

(human cells:*E. coli*) for 90 min at 37 °C or activated by Ca^{2+}-ionophore A23187 (0.5 µM) for 10 min at 37 °C, as indicated. After the incubation, the supernatants (2 ml) were removed from the cells and transferred to 3 ml of ice-cold methanol containing 10 µl of deuterium-labeled internal standards (200 nM d_8-5S-HETE, d_4-LTB$_4$, d_5-LXA$_4$, d_5-RvD2, d_4-PGE$_2$, and 10 µM d_8-AA) for quantification of generated LM. Deuterated and non-deuterated LM standards were purchased from Cayman Chemical/Biomol (Hamburg, Germany).

For experiments with MDM homogenates, cells in PBS pH 7.4 were scraped in the presence of 1 mM EDTA, counted, aliquoted (0.8×10^6 cells/ml) and sonified (3×15 s) on ice to lyse the cells. To these homogenates 2 mM $CaCl_2$ and 2 µM AA was added and samples were incubated for 10 min at 37 °C to induce LM formation. The reaction was stopped by addition of 2 ml of ice-cold methanol containing 10 µl of deuterium-labeled internal standards (see above).

Sample preparation for ultra performance liquid chromatography-tandem mass spectrometry (UPLC-MS–MS) analysis of fatty acid substrates and LM from intact cells and homogenates was performed as reported [28]. In brief, samples were kept at −20 °C for 60 min to allow protein precipitation, centrifuged (1200 g, 4 °C, 10 min), 9 ml acidified H_2O (pH 3.5) was added, and LM were separated by solid phase extraction. Solid phase cartridges (Sep-Pak® Vac 6 cc 500 mg/6 ml C18; Waters, Milford, MA) were equilibrated with 6 ml methanol and 2 ml H_2O prior sample loading onto columns. After washing with 6 ml H_2O and additional 6 ml *n*-hexane, LM were eluted using 6 ml methyl formiate. Finally, samples were brought to dryness using an evaporation system (TurboVap LV, Biotage, Uppsala, Sweden) and resuspended in 100 µl methanol–water (50/50, v/v) for UPLC-MS–MS automated injections. LM profiles were analyzed by means of an Acquity™ UPLC system (Waters, Milford, MA) and a QTRAP 5500 Mass Spectrometer (ABSciex, Darmstadt, Germany) equipped with a Turbo V™ Source and electrospray ionization (ESI) as reported [28]. Briefly, LM were separated using an ACQUITY UPLC® BEH C18 column (1.7 µm, 2.1 × 100 mm; Waters, Eschborn, Germany) at 50 °C with methanol–water–acetic acid of 42:58:0.01 (v/v/v) at a flow rate of 0.3 ml/min that was ramped to 86:14:0.01 (v/v/v) over 12.5 min and then to 98:2:0.01 (v/v/v) for 3 min. The QTrap 5500 was operated in negative ionization mode using scheduled multiple reaction monitoring (MRM) coupled with information-dependent acquisition. The scheduled MRM window was 60 s, optimized LM parameters were adopted [28], and the curtain gas pressure was set to 35 psi. The retention time and at least six diagnostic ions for each LM were confirmed by means of an external standard (Cayman Chemical/Biomol). Quantification was achieved by calibration curves for each LM. Linear calibration curves were obtained for each LM and yielded r^2

values of 0.998 or higher. Additionally, the limit of detection for each targeted LM was determined [28].

Flow cytometry

Fluorescent staining for flow cytometric analysis of MDM was performed in FACS buffer (PBS pH 7.4 containing 0.5% bovine serum albumin (BSA), 2 mM EDTA and 0.1% sodium azide). Non-specific antibody binding was blocked using mouse serum (10 min at 4 °C) prior to staining with antibodies. Then, MDM were stained with fluorochrome-labelled antibody mixtures (20 min at 4 °C). The following antibodies were used: FITC anti-human CD14 (clone M5E2), APC-H7 anti-human CD80 (clone L307.4, BD Bioscience, San Jose, CA), PE-Cy7 anti-human CD163 (clone RM3/1, Biolegend, San Diego, CA), APC anti-human VSIG-4 (clone JAV4), PerCP-eFluor710 anti-human CD206 (clone 19.2, eBioscience, San Diego, CA). Cells were resuspended in 300 µL FACS buffer containing propidium iodide staining solution (40 ng/test, eBioscience, San Diego, CA) to determine viability. Upon staining, MDM were analyzed using a FACS Canto Plus flow cytometer (BD Bioscience). FlowJo X Software (BD Bioscience) was used for data analysis.

Immunofluorescence microscopy

MDM (2×10^6 cells) were seeded onto glass coverslips in a 6-well plate (bottom compartment of Boyden chambers) and cultured for 48 h with or without A549 cells (2×10^6 cells; upper compartment) in presence of IL-4. MDM were separated from A549 cells, and *E. coli* (ratio 1:50, MDM:*E. coli*) or vehicle (PBS) were added at 37 °C. After 90 min incubation cells were fixed with 4% paraformaldehyde solution. Acetone (5 min, 4 °C) followed by 0.25% Triton X-100 for 10 min at RT was used for permeabilization before blocking with normal goat serum 10% (50062Z, Thermo Fisher). Samples were incubated with mouse monoclonal anti-5-LO antibody, 1:100 (6A12 AB, 250 µg/ml; kindly provided by Dr. Dieter Steinhilber, Goethe-University-Frankfurt, Frankfurt, Germany) and rabbit polyclonal antibodies against 5-LO-activating protein (FLAP), 5 µg/ml (ab85227, Abcam, Cambridge, UK), or mouse monoclonal anti-15-LO-1 antibody, 1:100 (ab119774, Abcam) and rabbit anti-5-LO antibody, 1:100 (1550 AK6, kindly provided by Dr. Olof Radmark, Karolinska Institutet, Stockholm, Sweden) at 4 °C overnight. 5-LO, 15-LO-1 and FLAP were stained with the fluorophore-labeled secondary antibodies: Alexa Fluor 488 goat anti-rabbit IgG (H+L), 1:500 (A11034, Thermo Fisher) and Alexa Fluor 555 goat anti-mouse IgG (H+L); 1:500 (A21424, Thermo Fisher). Nuclear DNA was stained with ProLong Gold Antifade Mountant with DAPI (15395816, Thermo Fisher). Samples were analyzed by a Zeiss Axiovert 200 M microscope, and a Plan Neofluar × 40/1.30 Oil (DIC III) objective (Carl Zeiss, Jena, Germany). An AxioCam MR camera (Carl Zeiss) was used for image acquisition.

SDS-PAGE and Western blot

Cell lysates of MDM (2×10^6 cells) were separated on 10% (5-LO, 15-LO-1, 15-LO-2, COX-2, cPLA$_2$-α, p38 mitogen-activated protein kinase (MAPK), phospho-p38 MAPK, extracellular signal-regulated protein kinase (ERK)-1/2, phospho-ERK-1/2), phospho-mitogen-activated protein kinase-activated protein kinase-2 (MAPKAPK-2, MK-2) and 16% (FLAP) polyacrylamide gels, and blotted onto nitrocellulose membranes (Amersham™ Protran Supported 0.45 µm nitrocellulose, GE Healthcare, Freiburg, Germany). Membranes were incubated with the following primary antibodies: rabbit polyclonal anti-5-LO, 1:1000 (by Genscript, Piscataway to a peptide with the C-terminal 12 amino acids of 5-LO: CSPDRIPNSVA; kindly provided by Dr. Marcia E. Newcomer, Louisiana State University, LA); mouse monoclonal anti-15-LO-1, 1:500 (ab119774, Abcam); rabbit polyclonal anti-15-LO-2, 1:200 (ab23691, Abcam); rabbit polyclonal anti-COX-2, 1:500 (4842, Cell Signaling, Danvers, MA); rabbit polyclonal anti-cPLA$_2$-α, 1:1000 (2832, Cell Signaling); rabbit monoclonal anti-p38 MAPK, 1:1000 (8690, Cell Signaling); rabbit polyclonal anti-phospho-p38 MAPK, 1:1000 (9211, Cell Signaling); rabbit monoclonal anti-ERK-1/2, 1:1000 (4695, Cell Signaling); mouse monoclonal anti-phospho-ERK-1/2, 1:750 (9106, Cell Signaling); rabbit monoclonal anti-phospho-MK-2, 1:1000, (3316, Cell Signaling), rabbit polyclonal anti-FLAP, 1:1000 (ab85227, Abcam); mouse monoclonal anti-β-actin, 1:1000 (3700, Cell Signaling); and rabbit monoclonal anti-GAPDH, 1:1000 (5174, Cell Signaling). Immunoreactive bands were stained with IRDye 800CW Goat anti-Rabbit IgG (H+L), 1:15,000 (926 32211, LI-COR Biosciences) and/or IRDye 680LT Goat anti-Mouse IgG (H+L), 1:40,000 (926–68020, LI-COR Biosciences), and visualized by an Odyssey infrared imager (LI-COR Biosciences, Lincoln, NE). Data from densitometric analysis were background corrected.

Ca²⁺ imaging

MDM (2×10^6 cells) were detached by scraping in the presence of 1 mM EDTA. Cells were centrifuged and resuspended in HEPES-buffer (135 mM NaCl, 5 mM KCl, 1 mM MgSO$_4$ × 7 H$_2$O, 0.4 mM KH$_2$PO$_4$, 5.5 mM glucose, 20 mM HEPES pH 7.4) containing 1 µM Fura-2-AM and kept for 30 min at 37 °C in the dark. Then, cells were washed and resuspended in HEPES-buffer containing 0.1% fatty acid-free BSA at a density of 0.75×10^6/ml. 200 µl of the cell suspension were transferred into a 96-well plate and 1 mM CaCl$_2$ was added. After 10 min,

E. coli (MDM:*E. coli* = 1:50) or vehicle (PBS) was added. The signal was monitored in a thermally (37 °C) controlled NOVOstar microplate reader [BMG Labtechnologies, Offenburg, Germany; emission at 510 nm, excitation at 340 nm (Ca^{2+}-bound Fura-2) and 380 nm (free Fura-2)]. After cell lysis with Triton X-100 the maximal fluorescence signals were monitored, and after chelating Ca^{2+} with 20 mM EDTA the minimal fluorescence signals were recorded. The ratio of signals obtained with Triton X-100 subtracted by the signals obtained at basal fluorescence intensity (shown as Δratio) of each experiment was set to 100%. Ca^{2+}-influx was calculated by determining the area under the curve (AUC) for Δratio of *E. coli* stimulation subtracted by AUC of PBS-control (AUC $_{E.coli}$ − AUC$_{PBS}$) after 90 min.

Statistical analysis

The sample size for experiments was chosen empirically based on previous studies [27, 29] to ensure adequate statistical power. Results are expressed as mean ± standard error of the mean (S.E.M) of n observations, where n represents the number of experiments with cells from separate donors, performed on different days in simplicates or duplicates, as indicated. Analysis of data were conducted using Graph-Pad Prism 8 software (San Diego, CA). T-test was used for comparison of two groups. Two-way ANOVA was used for statistical analysis in case of two different categorical independent variables influence one continuous dependent variable, as indicated. The criterion for statistical significance is $P < 0.05$.

Results

Coculture of MDM during alternative activation with A549 cells primes for elevated LM biosynthesis

In vitro, M2-like TAM can be obtained from MDM after differentiation of blood monocytes with M-CSF and subsequent alternative activation with Th2-related IL-4 [30]. Human monocytes were first differentiated with M-CSF for 6 days to obtain mature MDM, which were then treated with IL-4 for 48 h towards TAM/M2-like MDM in the absence ("MDM") or presence of the human alveolar basal epithelial cancer cell line A549 ("MDM$_{A549}$") in trans-well Boyden chambers. Under these conditions, the two cell types are able to communicate via secreted molecules but without direct cell–cell contacts (Fig. 1a). After separation from A549 cells, the MDM were analyzed by flow cytometry for expression of surface markers that are characteristic for TAM/M2-like macrophage phenotypes. In agreement with the literature [30], the M2-markers CD163 and CD206 are strongly expressed in MDMs when treated with IL-4 in contrast to the M1-like markers CD80 and V-set immunoglobulin-domain-containing 4 (VSIG-4), a B7 family-related protein that is expressed by resting macrophages [31]. Cocultivation with
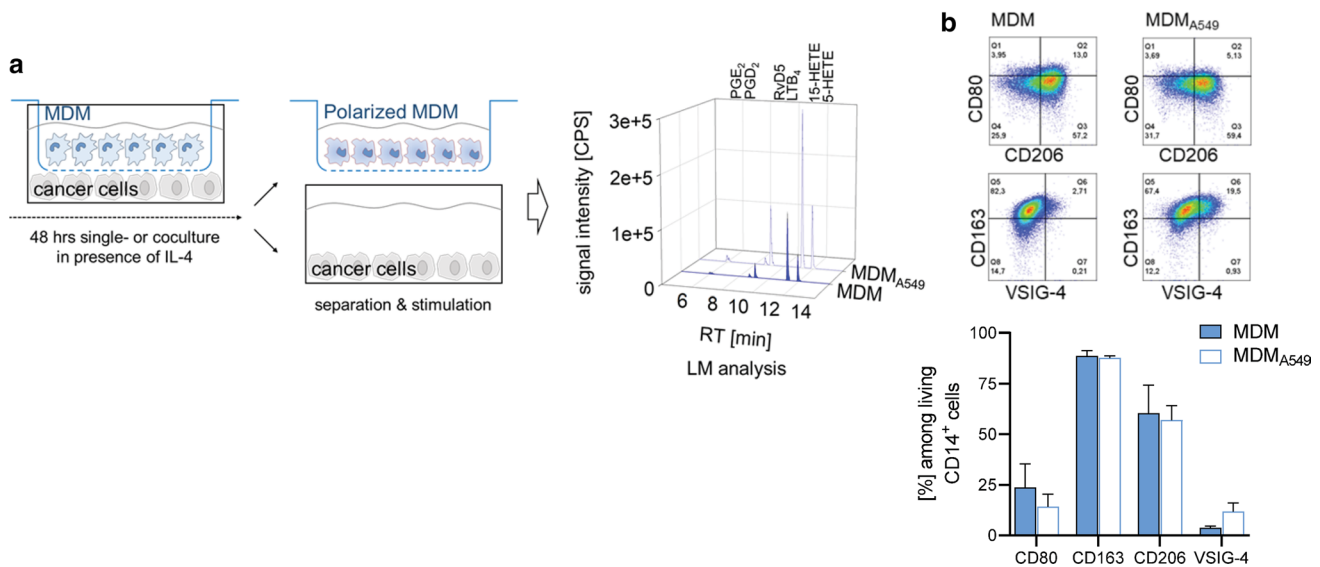

Fig. 1 MDM-cancer cell coincubation system without direct cell–cell contacts. **a** Using a Boyden chamber, MDM are cocultured with cancer cells, separated by a semipermeable membrane to avoid cell–cell contacts, in the presence of IL-4 for 48 h. Then, the MDM and cancer cells are separately challenged with *E. coli* (O6:K2:H1; ratio = 1:50) for another 90 min. LM released into the supernatants were analyzed via UPLC-MS–MS reflected by the chromatograms (retention times:

PGE$_2$, 6.0 min; RVD5, 8.8 min; LTB$_4$ 9.2 min; 15-HETE, 11.4 min; 5-HETE 12.0 min). **b** Effect of A549 cancer cells on IL-4-polarized MDM phenotypic surface markers. Expression of surface markers CD80, CD206, CD163 and VSIG-4 were determined by flow cytometry; representative pseudocolor dot plots from n = 3 separate donors; quantification is given as bar charts, data are means ± S.E.M

A549 cells during IL-4 treatment was without substantial effect on the expression of CD163 and CD206 on MDM, while CD80 expression was slightly decreased and VSIG-4 expression increased (Fig. 1b).

Alternative activation of human MDM by IL-4 is strikingly associated with the expression of phenotype-specific LM-biosynthetic pathways [27, 28, 32]. Exposure of IL-4-activated macrophages by an appropriate stimulus such as pathogenic bacteria (e.g., *E. coli*) induces the generation of broad spectrum bioactive LM [27, 28]. These LM encompass pro-tumoral COX-derived PG and 5-LO-derived LT and 5-HETE [16–18] but also anti-tumoral SPM that suppress tumor growth [21] and stimulate resolution in cancer [22]. Note that besides pathogenic bacteria, other relevant stimuli, in particular related to cancer, failed to induce substantial and broad spectrum LM formation in M2 macrophages in vitro [27], although this macrophage subtype is considered as a major source of LM in vivo. Coincubation with A549 cells during MDM activation by IL-4 for 48 h strongly elevated that capacity of the MDM to produce bioactive 5-LO products (e.g., LTB_4 and 5-HETE) upon subsequent activation by pathogenic *E. coli* (Fig. 2a, b and Online Resource 1). Also the capacities to generate COX products and 15-LO-derived LM, including SPM, namely RvE3, RvD2 and RvD5, were increased in these MDM due to preceding coculture with A549 cells, however, with lower magnitudes (Fig. 2a). Obviously, LM that require both 5-LO and 15-LO activities such as 5,15-diHETE or LXA_4 were also prominently increased.

To prove that the MDM-modulating effects of the A549 cancer cells are not just the consequence of coculture with any adherent cell-type in an unspecific manner, we used HUVEC which are adherent endothelial cells that produce COX- and LO-derived LM from various fatty acid substrates [33] but are not transformed into cancerous cells. In contrast to A549 cells, cocultivation of MDM with the non-transformed HUVEC failed to increase 5-LO and COX product formation upon subsequent exposure to *E. coli*, except for $PGF_{2\alpha}$. The formation of 15-LO-derived SPM and their monohydroxy precursors was rather impaired due to preceding HUVEC coculture (Fig. 2a). Besides A549 cells, we also coincubated MDM during IL-4 activation with two other cancer cell lines, namely the human colon epithelial cancer cell line HT-29 and promyelocytic leukemia HL60 cells. Coculture with HT-29 increased COX and 5-LO product formation in MDM but without consistent modulation of 15-LO activities. In contrast, HL60 cells failed to promote LM biosynthesis in MDM but rather suppressed it (Fig. 2a). Note that coculture with all three cancer cell lines (A549, HT-29 and HL60) slightly increased the release of free fatty acids (mainly AA) to a similar degree (Fig. 2a). It is therefore unlikely that the pronounced differences in LM profiles originate from altered release of fatty acids as substrates for LM biosynthesis but are rather due to favorable effects of A549 cells on the enzymatic transformation of the substrates by the LM-biosynthetic enzymes in MDM.

Influence of A549 cell coculture on the protein expression of LM-biosynthetic enzymes in MDM

The increased capacities of IL-4-activated MDM to generate LM due to precedent coculture with A549 cells could be related to higher protein contents of the LM-biosynthetic enzymes. Western blot analysis of total cell lysates of MDM cultivated with IL-4 for 48 h revealed equal protein levels of COX-2, 5-LO and its helper protein FLAP, and 15-LO-2 for cells grown in the absence or presence of A549 cells (Fig. 2c). In agreement with others [34], mPGES-1 was not expressed in these IL-4-treated MDM, and the low levels of COX-1 (not shown) were inconsistently detectable. Surprisingly, the amounts of $cPLA_2$-α protein were much reduced when MDM were cocultured with A549 cells as compared to MDM monocultures (Fig. 2c), although the capacity to liberate AA for LM formation was rather elevated under these conditions (see Fig. 2a). On the other hand, for expression of 15-LO-1, a tendency towards higher protein levels was appreciable when MDM were cocultured with A549 (Fig. 2c), which might explain the higher levels of 15-LO products including SPM (see Fig. 2a, b).

In addition, we studied LM production in MDM homogenates prepared by sonification using a well-established cell-free assay [35] as measure for the amounts of enzymatically active COX-2, 5-LO, and 15-LO. Note that under these assay conditions, cellular regulatory mechanisms (e.g., phosphorylation or interaction with helper proteins) are not operative and substrate fatty acids must be supplied exogenously to ensure full activities of the enzymes. In line with the protein expression, the amounts of LM formed by COX-2, 5-LO and 15-LO did not substantially differ between MDM homogenates derived from monocultures and MDM/A549 cocultures (Fig. 2d), which indicates that the amounts of enzymatically active enzymes are comparable. Together, these data suggest that the marked increase of LM in MDM cocultured with A549 is not primarily caused by altered levels of the major LM-biosynthetic enzymes.

Coculture of MDM with A549 cells primes for activation of the p38 MAPK/MK-2 pathway that mediates increased 5-LO product synthesis

The lack of an increase in 5-LO and FLAP protein levels in MDM cocultured with A549 cells suggest that boosting of favorable regulatory mechanisms in the MDM may account for elevated 5-LO-derived LM. Cellular 5-LO activation is complex and depends on multiple factors including elevated intracellular Ca^{2+} levels ($[Ca^{2+}]_i$), 5-LO subcellular
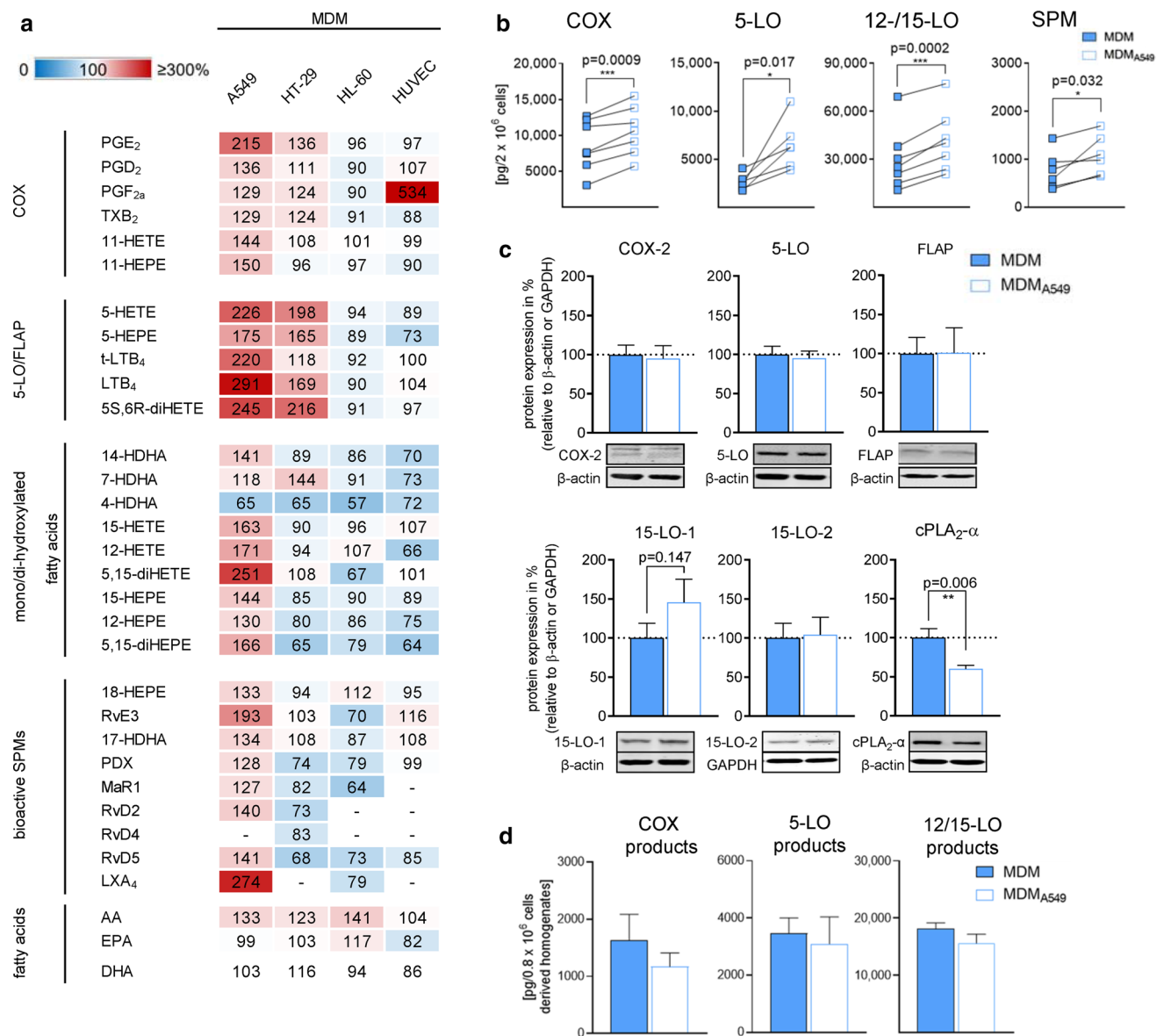
Fig. 2 Coculture of MDM during alternative activation with A549 cells primes for elevated LM biosynthesis. MDM were cocultured with either A549 cells, HT-29 cells, HL-60 cells or HUVEC in the Boyden chamber (see Fig. 1a) for 48 h in the presence of IL-4. **a, b** MDM were separated and challenged with *E. coli* (O6:K2:H1; ratio = 1:50) for 90 min at 37 °C. LMs were extracted and analyzed by UPLC-MS–MS. **a** Changes in LM formation of MDM after precedent coculture, given in percentage, versus LM produced in MDM after monocultures (= 100%, white) upon subsequent exposure to *E. coli*. Data are shown in a heatmap and given as means, $n = 3–7$. **b** Absolute amounts of LM (COX products, 5-LO products, 12/15-LO products and SPM) produced in MDM after coculture with A549 cells and in MDM after monocultures and subsequent exposure to *E. coli*, each, given in pg/2 × 10^6 MDM. Data are means, $n = 6–7$. *$P < 0.05$, **$P < 0.01$, ***$P < 0.001$, two-tailed t test. **c** MDM were analyzed for protein expression of COX-2, 5-LO, FLAP, 15-LO-1, 15-LO-2 and cPLA$_2$-α, as indicated, by Western blot, normalized to β-actin or GAPDH. Western blots are shown as representatives and data are means ± S.E.M., $n = 7–13$ separate donors; **$P < 0.01$, two-tailed t test, monocultures (100%) versus cocultures. **d** MDM in PBS containing 1 mM EDTA were sonified on ice and resulting homogenates, corresponding to 8 × 10^5 cells, were incubated with 2 μM AA and 2 mM CaCl$_2$ for 10 min at 37 °C. LM were extracted and analyzed by UPLC-MS–MS. Data are means ± S.E.M, $n = 3$

localization and interaction with FLAP, and phosphorylation of 5-LO by mitogen-activated protein kinase-activated protein kinase (MAPKAPK, MK)-2 and ERK-1/2 [36].

First, we analyzed the $[Ca^{2+}]_i$ in MDM upon exposure to *E. coli* which was shown to be elevated under such conditions leading to LM formation [27]. Preceding coculture with A549 cells slightly increased the $[Ca^{2+}]_i$ in MDM exposed to *E. coli* for 90 min (Fig. 3a), which is considered as the onset of 5-LO product formation under these conditions [27]. Moreover, the subcellular redistribution of 5-LO
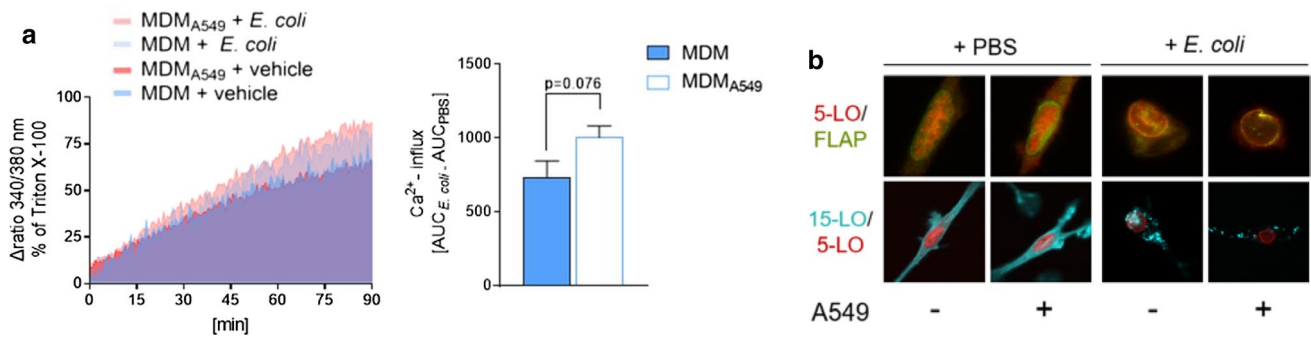
Fig. 3 Influence of A549 cell coculture on the mobilization of $[Ca^{2+}]_i$ and LO translocation in MDM. MDM were cocultured with A549 cells or kept in monocultures in a Boyden chamber (see Fig. 1a) for 48 h in the presence of IL-4 and separated from A549 cells. **a** Measurement of $[Ca^{2+}]_i$ in Fura-2-AM-loaded MDM resuspended in HEPES-BSA buffer containing 1 mM Ca^{2+} and exposed to *E. coli* (O6:K2:H1; ratio = 1:50) or PBS (vehicle) at 37 °C for up to 90 min. The ratio of absorbance at 340 vs. 380 nm reflecting $[Ca^{2+}]_i$ of MDM stimulated with *E. coli* versus unstimulated cells over 90 min (left panel). Data are given as AUC of MDM stimulated with *E. coli* subtracted by the AUC of unstimulated MDM (right panel), means ± S.E.M., $n = 3$ separate donors. Two-tailed t test. **b** MDM were challenged with *E. coli* (O6:K2:H1; ratio = 1:50) or PBS (vehicle) for 90 min at 37 °C. MDM on cover slips were fixed, permeabilized, stained with antibodies against 5-LO (red), FLAP (green), and 15-LO-1 (cyan-blue), and then analyzed by immunofluorescence microscopy. Scale bars = 10 μm (upper panel), 20 μm (lower panel). Results shown for single cells are representative for approx. 100 individual cells analyzed in $n = 3$ independent experiments

determines the capacity of various leukocytes to produce 5-LO products, with intranuclear 5-LO being favorable in this respect [36]. Immunofluorescence microscopy showed a similar subcellular localization of 5-LO in IL-4-treated MDM independent on whether A549 cells were present, both, in unstimulated and *E. coli*-activated cells (Fig. 3b).

Next, we assessed if preceding coculture of IL-4-treated MDM with A549 cells influences the activation of MK-2 and ERK-1/2 upon MDM activation by *E. coli*. Exposure of MDM to *E. coli* increased the phosphorylation/activation of MK-2 within 10–30 min which was maintained up to 90 min (Fig. 4a). Without preceding A549 cell coculture, MK-2 phosphorylation was elevated after 10 min of exposure to *E. coli* and declined again at 90 min, whereas the upstream p38 MAPK was only transiently activated in MDM after 30 min (Fig. 4a). After coculture of MDM with A549 cells and stimulation with *E. coli*, both MK-2 and p38 MAPK phosphorylation were instead strongly increased at 10–30 min (Fig. 4a). In contrast, ERK-1/2 phosphorylation was not enhanced by *E. coli* in IL-4-activated MDM, and coculture with A549 cells was without further effect (Fig. 4a).

Finally, we used the selective p38 MAPK inhibitor Skepinone-L [37] to investigate if the blockade of the p38 MAPK/MK-2 pathway would indeed reverse the 5-LO-stimulatory impact of A549 cells on IL-4-treated MDM. Formation of 5-LO-derived LM (such as LTB$_4$) in *E. coli*-stimulated MDM from cocultures with A549 was efficiently suppressed by Skepinone-L (down to 30%, Fig. 4b and Online Resource 2). Neither COX products nor purely 15-LO-derived LM were markedly impaired by Skepinone-L, while 5-LO/15-LO-derived products were either diminished (LXA$_4$) or

hardly affected (Fig. 4b and Online Resource 2). Note that Skepinone-L also suppressed 5-LO product formation in *E. coli*-stimulated MDM that were grown in the absence of A549, as expected [38, 39], but the magnitude of inhibition was less pronounced (50% of the 5-LO products remained, Fig. 4b and Online Resource 2). Together, our data suggest that the strong upregulation of 5-LO product formation in MDM due to coculture with A549 cells is caused by priming the p38 MAPK/MK-2 pathway that upon subsequent stimulation by *E. coli* is strongly activated and thus stimulates 5-LO activity.

Coculture of A549 cells with MDM increases COX-2 expression and prostanoid formation

Increased formation of eicosanoids in cancer was reported by many studies before [16–18]. Here, we assessed whether MDM could alter LM biosynthesis in A549 cells using the same coculture model from above. Exposure of A549 cells to *E. coli* caused marked formation of COX products, but in contrast to IL-4-treated MDM, A549 cells failed to produce appreciable amounts of 5-LO and 15-LO products (Fig. 5a). When A549 cells were cocultured with MDM for 48 h and then exposed to *E. coli*, a marked elevation of COX products (i.e., PGE$_2$, PGD$_2$, PGF$_{2\alpha}$, TxB$_2$) was evident (Fig. 5a, b). The minute amounts of other LM that could be detected (i.e., 5-HETE, 5-HEPE, 4-HDHA, 18-HEPE) were not significantly increased, except for 15-HETE (Fig. 5a), which might be a COX product [40]. Interestingly, the release of AA as COX substrate was rather decreased in A549 due to MDM coculture. Since *E. coli* might constitute, in contrast to MDM, a suboptimal stimulus for non-immune A549 cells,
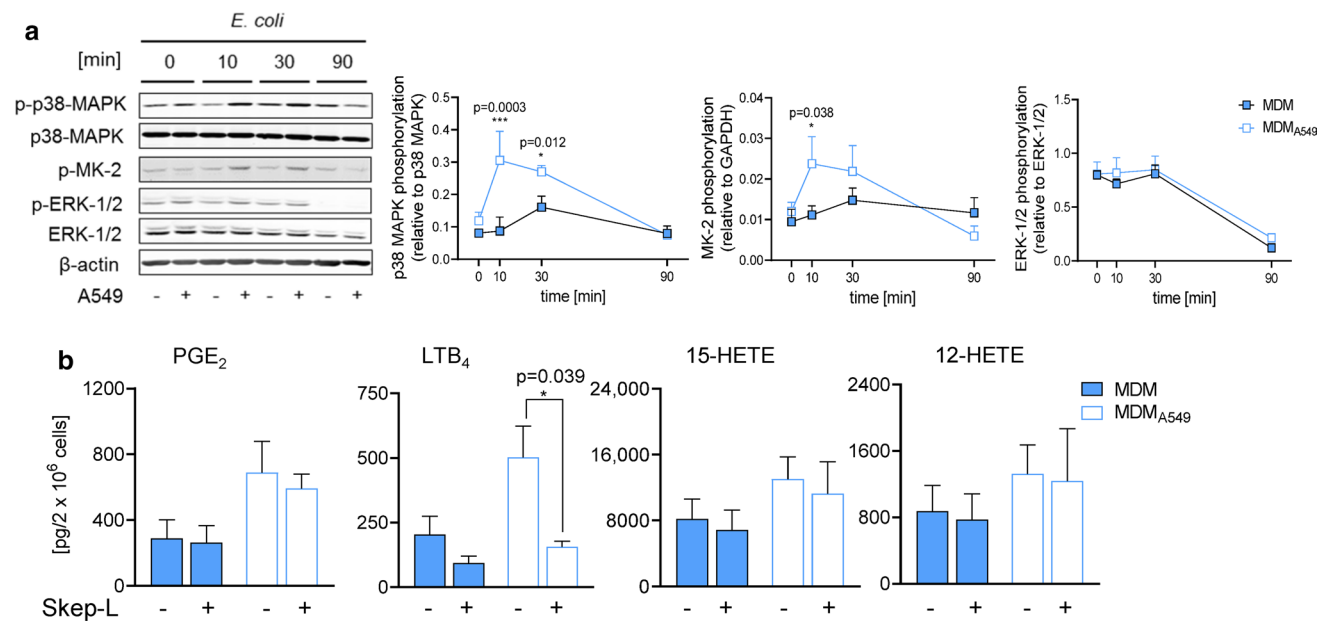
Fig. 4 Coculture of MDM with A549 cells primes for activation of the p38 MAPK/MK-2 pathway that mediates increased 5-LO product synthesis. MDM were cocultured with A549 cells or kept in monocultures in a Boyden chamber (see Fig. 1a) for 48 h in the presence of IL-4. **a** MDM were separated and exposed to *E. coli* (O6:K2:H1; ratio = 1:50) for the indicated times. Cell lysates were prepared and immunoblotted for phospho-p38 MAPK, p38 MAPK, phospho-ERK-1/2, ERK-1/2, phospho-MK2, and normalized to β-actin or GAPDH for densitometric analysis. Data are means ± S.E.M., $n = 3$ separate donors. **b** MDM were preincubated for 15 min with 0.3 μM Skepinone-L or 0.1% DMSO (vehicle) and exposed to *E. coli* (O6:K2:H1; ratio = 1:50) for 90 min at 37 °C. LMs were extracted and analyzed by UPLC-MS–MS. Absolute amounts (pg/2 × 10^6 MDM) of selected LM (PGE$_2$, LTB$_4$, 15-HETE and 12-HETE) are shown as bar charts. Data are means, $n = 3$. *$P < 0.05$, two-way ANOVA followed by Tukey post-hoc test

we also used the Ca^{2+}-ionophore A23187, a well-recognized stimulus for 5-LO/COX product formation, to induce COX product biosynthesis. Again, the formation of various PGs, particularly PGE$_2$, was strongly increased when A549 were cocultured with IL-4-activated MDM prior to *E. coli* stimulation (Fig. 5c). To elucidate the reason behind the increased COX product levels, we analyzed the expression of COX-2, an inducible enzyme during inflammation and cancer [17], in A549 cells by Western blot. Coculturing with MDM clearly increased COX-2 protein levels in A549 cells (Fig. 5d). Note that IL-4-activated MDM also increased PG formation in HT-29 cells, although less pronounced as in A549 cells, while HUVEC were not affected in this respect (Fig. 5e and Online Resource 3).

Discussion

Here we show that the communication between MDM and epithelial cancer cells without direct contacts modifies the capabilities of both cell types to produce LM that are of relevance for tumor biology. Thus, A549 or HT-29 epithelial cancer cells prompt MDM to increase the formation of a broad variety of LM and the release of the fatty acid substrate AA. In particular, various 5-LO-derived LM including LTB$_4$, 5-HETE, LXA$_4$ and 5,15-diHETE were markedly elevated, likely due to upregulation of the p38 MAPK/MK-2 pathway known to activate 5-LO [38, 39]. Of note, coculture of MDM with non-tumorigenic HUVEC cells or with leukemic HL60 cells failed in this respect, implying cell type-selective communication via signals secreted from epithelial cancer cells. Conversely, MDM prompt epithelial cancer cells (but not HUVEC) for increased COX-2 expression along with elevated PG levels upon subsequent stimulation. Since both LT and PG promote all stages of cancer development [17, 18], our findings reveal a potential mechanism of how cancer cells exploit the communication with TAM to boost the formation of pro-tumoral mediators in the TME for effectively promoting tumorigenesis.

Tumors consist of cancer cells and surrounding stromal cells that intensively communicate, forming the TME, where TAM play crucial roles in supporting all hallmarks of cancer [41]. LM are often formed by transcellular metabolism in a coordinated effort by multiple cell types [25]. Thus, cancer cells, with often overexpressed COX/5-LO pathways [17], may accomplish the generation of elevated and tumor-specific LM profiles in conjunction with eicosanoid-producing TAM in the TME. LM profiling of the TME using an orthotopic model of murine lung cancer revealed increased COX- and 5-LO-derived LM during tumor progression [42].
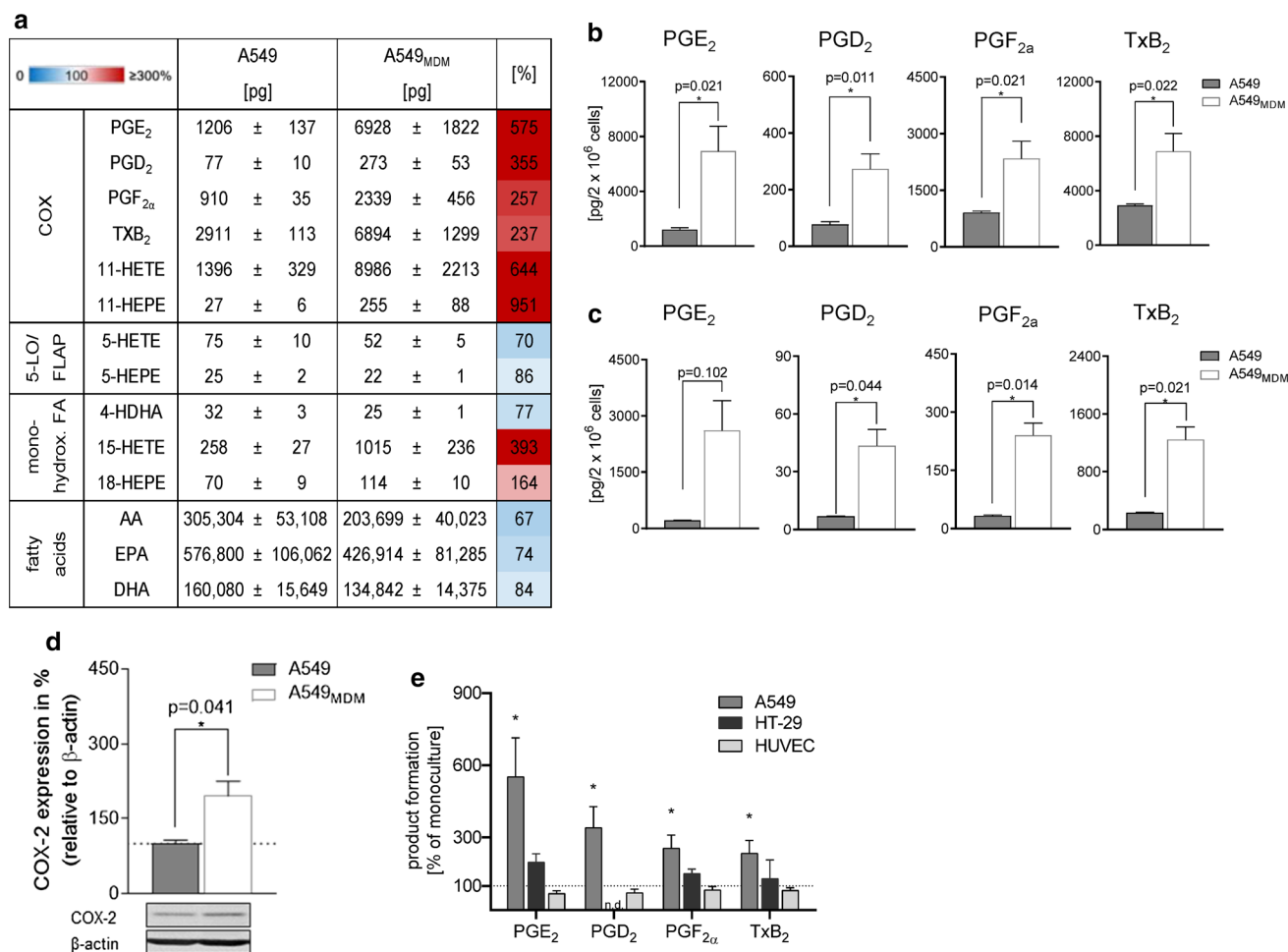
a

		A549 [pg]			A549$_{MDM}$ [pg]			[%]
COX	PGE$_2$	1206	±	137	6928	±	1822	575
	PGD$_2$	77	±	10	273	±	53	355
	PGF$_{2\alpha}$	910	±	35	2339	±	456	257
	TXB$_2$	2911	±	113	6894	±	1299	237
	11-HETE	1396	±	329	8986	±	2213	644
	11-HEPE	27	±	6	255	±	88	951
5-LO/FLAP	5-HETE	75	±	10	52	±	5	70
	5-HEPE	25	±	2	22	±	1	86
mono-hydrox. FA	4-HDHA	32	±	3	25	±	1	77
	15-HETE	258	±	27	1015	±	236	393
	18-HEPE	70	±	9	114	±	10	164
fatty acids	AA	305,304	±	53,108	203,699	±	40,023	67
	EPA	576,800	±	106,062	426,914	±	81,285	74
	DHA	160,080	±	15,649	134,842	±	14,375	84

Fig. 5 Coculture of A549 cells with MDM increases COX-2 expression and prostanoid formation. A549 cells were cocultured with MDM or kept in monocultures in a Boyden chamber (see Fig. 1a) for 48 h in the presence of IL-4. **a, b** A549 cells were separated from MDM and challenged with *E. coli* (O6:K2:H1; ratio = 1:50) for 90 min at 37 °C. Then LM were extracted and analyzed by UPLC-MS–MS. **a** Data for all detectable LM are given as absolute amounts (pg/2 × 10^6 A549 cells, means ± S.E.M., $n = 4$) and as percentage of A549 cocultures with MDM versus A549 monocultures (= 100%), shown in a heatmap. **b** Absolute amounts (pg/2 × 10^6 MDM) of PG shown as bar charts. Data are means ± S.E.M., $n = 4$. *$P < 0.05$, two-tailed *t* test. **c** A549 cells were separated from MDM and challenged with 0.5 μM Ca^{2+}-ionophore A23187 for 10 min at 37 °C. Then LM were extracted and analyzed by UPLC-MS–MS. Data are given as pg/2 × 10^6 A549 cells, means ± S.E.M., $n = 3$. **d** A549 cells were separated and analyzed for protein expression of COX-2 by Western blot, normalized to β-actin. Western blots are shown as representatives and data are given as means ± S.E.M., $n = 6$–10 separate donors; *$P < 0.05$, monocultures (100%) versus cocultures, two-tailed *t* test. **e** A549 cells, HT-29 cells or HUVEC were cocultured with MDM or kept in monocultures, each, in the Boyden chamber (see Fig. 1a) for 48 h in the presence of IL-4. A549 cells, HT-29 cells or HUVEC were separated from MDM and challenged with *E. coli* (O6:K2:H1; ratio = 1:50) for 90 min at 37 °C. Then PG were extracted and analyzed by UPLC-MS–MS. Changes in PG formation in A549 cells, HT-29 cells or HUVEC after precedent coculture with MDM, given in percentage versus LM produced in monocultures (= 100%), upon subsequent exposure to *E. coli*. Data are means ± S.E.M., $n = 3$–4 separate donors; *$P < 0.05$, two-tailed *t* test

The primary aim of the present study, however, was not to simply establish LM profiles, which are produced by MDM/cancer cell cocultures and characterize the TME, but rather to investigate how the communication of these cells without contacts would affect the acquired capabilities to generate LM via secreted signals in the respective cell type.

The formation of all COX-, 5-LO- and 12/15-LO-derived LM in MDM were increased upon coculture with A549 cells versus MDM monocultures. However, among the major LM-biosynthetic enzymes/proteins in MDM, coculture with A549 cells did not alter the protein levels of COX-2, 5-LO, FLAP, and 15-LO-2, and upregulated 15-LO-1 protein expression only by trend, whereas cPLA$_2$-α was markedly downregulated. This indicates that except for 15-LO products, alterations in enzyme expression levels play a subordinated role for LM elevation in our coculture model. Also, the moderately increased AA supply is likely not causative, since (1) coculture with HL-60 caused even more robust

AA release without elevation of LM, and (2) also DHA- and EPA-derived LM were increased without concomitant elevation of these fatty acids. Rather stimulatory mechanisms of the respective enzymes are operative, in particular for 5-LO that is highly susceptible to cellular regulatory mechanisms controlling its activity [36].

5-LO and its products including LTB_4, cys-LTs and 5-HETE affect cancer cell proliferation, angiogenesis, survival and metastasis, and the 5-LO protein was found to be overexpressed in cancers of colon, breast, pancreas, prostate, lung and in glioblastomas [23, 24]. Although cancer cells derived from 5-LO-negative progenitor epithelial cells may acquire 5-LO expression, and thus the capability for LT formation [43, 44], A549 cells in our hands produced no appreciable amounts of 5-LO products. Recent studies showed that the prime source of the substantially elevated LTB_4 levels in lung tumor metastases are 5-LO-positive infiltrating neutrophils [20], monocytic cells [45], or alveolar macrophages [46]. Also, in a murine model of colon polyposis, mast cells were revealed as major source of pro-tumorigenic 5-LO [47], and in ovarian cancer 5-LO expression and levels of 5-LO-derived LM correlated with TAM infiltration [48]. Although 5-LO-derived LM create a pro-inflammatory TME promoting tumorigenesis [23, 24], they can also attract cytotoxic T cells and therefore exhibit anti-tumorigenic potential [49].

Our data provide mechanistic insights into how cancer cells might elevate LT biosynthesis in 5-LO-expressing TAM of the TME. Ringleb et al. showed that MCF-7 breast epithelial cancer cells downregulate 5-LO activity in human TAM-like MDM, which however, required MCF-7 cell death and direct contact with MDM, resulting in the blockade of 5-LO transcription [50]. In our study, 5-LO protein expression in MDM was unaltered after coculture with A549 cells, which were viable and were separated from MDM (devoid of direct contacts). Moreover, crude 5-LO activity in homogenates was unaffected by preceding coculture with A549 cells, suggesting that the amounts of enzymatically active 5-LO in the intact MDM are unaffected. Instead, coculture with A549 facilitated the activation of the p38 MAPK/MK-2 pathway in MDM upon subsequent stimulation. p38 MAPK is the upstream activator of MK-2 that in turn phosphorylates 5-LO at Ser-271 [51], which increases cellular 5-LO product formation [39]. In agreement with previous results [38], pharmacological inhibition of the p38 MAPK/MK-2 using the highly selective p38 MAPK inhibitor Skepinone-L [37] blocked the stimulatory effect of A549 in MDM. Note that Skepinone-L only marginally inhibited the formation of other LM in MDM, such as COX-derived PGs or SPMs, the latter being essentially produced by 15-LO-1 in *E. coli*-stimulated MDM [27]. Activation of ERK-1/2, another 5-LO-activating kinase [52], was not affected in contrast to p38 MAPK/MK-2. Significant upregulation of

other 5-LO-stimulatory events such as increase of $[Ca^{2+}]_i$ or enhanced 5-LO nuclear translocation [36] were not immediately evident. Conclusively, epithelial cancer cells, but not leukemic HL-60 cells or HUVEC, release or deplete specific factor(s) which are responsible for activation of the p38 MAPK/MK-2 pathway during coculture with MDM, leading to marked 5-LO activity in response to external stimulation.

$cPLA_2$-α is a major enzyme in macrophages responsible for the release of AA, which is converted as COX/LO substrate to eicosanoids [53]. Of interest, $cPLA_2$-α expression was significantly downregulated in MDM when cocultured with A549 cells. Despite the low $cPLA_2$-α protein levels, these MDM even surpassed MDM monocultures with greater $cPLA_2$-α amounts in AA supply and AA-derived LM biosynthesis upon *E. coli* exposure. Since p38 MAPK signaling not only induces 5-LO activation but also can increase $cPLA_2$-α activity and AA release in macrophages [54], we speculated that the higher AA supply in MDM after coculture with A549 cells might depend on the activation of p38 MAPK/MK-2. However, Skepinone-L failed to block the upregulated AA release in contrast to 5-LO product formation, which suggests that alternative pathways of $cPLA_2$-α activation [53] or possibly other PLA_2 isoforms [55] dominate fatty acid release under these conditions.

Besides PGs and LTs, also SPM must be considered as LM with relevance for tumorigenesis with, however, overall anti-tumoral features [56]. 15-LO-1 is crucial for SPM formation in M2-like MDM [27] and considered to suppress cancer, likely by attenuating inflammation-driven carcinogenesis [57]. 15-LO-1 is commonly downregulated in cancer cells [57] implying reduced capacities for SPM formation. In our hands, 15-LO-1, but not 15-LO-2, was increased by trend in MDM after coculture with A549 cells, and higher levels of 15-LO-derived monohydroxylated AA and DHA products as well as SPM were produced versus MDM from monocultures. Interestingly, 15-HETE secretion from TAMs isolated from renal cell carcinoma was also higher versus normal kidney tissue, albeit in this case the 15-LO-2 pathway was seemingly operative [58].

The LM profile produced by stimulated A549 cells upon coculture with MDM revealed a selective and sustained elevation of the COX-2 pathway with tremendously elevated PGE_2 levels. PGE_2 was also most prominently increased among prostanoids in MDM cocultured with A549 cells. COX-2 is frequently expressed in many types of cancers with a multifaceted role in genesis or promotion of carcinogenesis by supporting apoptotic resistance, proliferation, angiogenesis, inflammation, invasion, and metastasis of cancer cells [59]. Animal studies confirmed the association of genetic COX-2 overexpression with tumorigenesis and malignant progression [60]. Among the COX-derived LM, especially PGE_2 and thromboxanes have been implicated in tumorigeneses and cancer [61]. PGE_2 stimulates tumor epithelial cells

by activating epidermal growth factor receptor (EGFR) and fibroblast growth factor receptor (FGFR)2 signaling, by activating the Ras/ERK-1/2, glycogen synthase kinase (GSK)-3β-catenin, and PI3K/Akt/peroxisome proliferator-activated receptor (PPAR)δ pathways, and by upregulation of Bcl-2, NF-κB, MMP2, and CCR7 [17]. In view of the strikingly increased formation of PG by A549 cells our data warrant further investigations aiming at identifying the molecular signals derived from MDM and elucidating the intracellular mechanisms that cause COX-2 upregulation. Potential candidates might be EGF and VEGF that are known to be released from M2-like TAM and in turn can induce COX-2 transcription [59, 62, 63].

Taken together, we showed here how the communication between human TAM-like MDM and epithelial cancer cells in cocultures dictate the acquirement of cell type-specific patterns of aberrant LM-biosynthetic pathways with potential consequences for tumorigenesis. Targeting bioactive lipids within the tumor and surrounding TME is eventually considered as a novel therapeutic approach for treating cancer patients [56]. Our results support such strategy for intervention with tumors by revealing that the formation of cancer-affecting LM is enhanced through contact-independent interactions between cancer cells and MDMs.

Compliance with ethical standards

Conflict of interest The authors declare that they have no conflict of interest.

References

1. Balkwill FR, Capasso M, Hagemann T (2012) The tumor microenvironment at a glance. J Cell Sci 125:5591–5596
2. Biswas SK, Allavena P, Mantovani A (2013) Tumor-associated macrophages: functional diversity, clinical significance, and open questions. Semin Immunopathol 35:585–600
3. Goswami KK, Ghosh T, Ghosh S, Sarkar M, Bose A, Baral R (2017) Tumor promoting role of anti-tumor macrophages in tumor microenvironment. Cell Immunol 316:1–10
4. Prenen H, Mazzone M (2019) Tumor-associated macrophages: a short compendium. Cell Mol Life Sci 76:1447–1458
5. Allavena P, Sica A, Garlanda C, Mantovani A (2008) The Yin-Yang of tumor-associated macrophages in neoplastic progression and immune surveillance. Immunol Rev 222:155–161
6. Biswas SK, Mantovani A (2010) Macrophage plasticity and interaction with lymphocyte subsets: cancer as a paradigm. Nat Immunol 11:889–896
7. Murakami M (2011) Lipid mediators in life science. Exp Anim 60:7–20
8. Calder PC (2006) Polyunsaturated fatty acids and inflammation. Prostaglandins Leukot Essent Fatty Acids 75:197–202
9. Funk CD (2001) Prostaglandins and leukotrienes: advances in eicosanoid biology. Science 294:1871–1875
10. Serhan CN (2014) Pro-resolving lipid mediators are leads for resolution physiology. Nature 510:92–101
11. Serhan CN, Levy BD (2018) Resolvins in inflammation: emergence of the pro-resolving superfamily of mediators. J Clin Invest 128:2657–2669
12. Hanahan D, Weinberg RA (2011) Hallmarks of cancer: the next generation. Cell 144:646–674
13. Mantovani A, Allavena P, Sica A, Balkwill F (2008) Cancer-related inflammation. Nature 454:436–444
14. Crusz SM, Balkwill FR (2015) Inflammation and cancer: advances and new agents. Nat Rev Clin Oncol 12:584–596
15. Greene ER, Huang S, Serhan CN, Panigrahy D (2011) Regulation of inflammation in cancer by eicosanoids. Prostaglandin Other Lipid Mediat 96:27–36
16. Nie D, Honn KV (2002) Cyclooxygenase, lipoxygenase and tumor angiogenesis. Cell Mol Life Sci 59:799–807
17. Wang D, Dubois RN (2010) Eicosanoids and cancer. Nat Rev Cancer 10:181–193
18. Greenhough A, Smartt HJ, Moore AE, Roberts HR, Williams AC, Paraskeva C, Kaidi A (2009) The COX-2/PGE2 pathway: key roles in the hallmarks of cancer and adaptation to the tumour microenvironment. Carcinogenesis 30:377–386
19. Kim W, Son B, Lee S, Do H, Youn B (2018) Targeting the enzymes involved in arachidonic acid metabolism to improve radiotherapy. Cancer Metastasis Rev 37:213–225
20. Wculek SK, Malanchi I (2015) Neutrophils support lung colonization of metastasis-initiating breast cancer cells. Nature 528:413–417
21. Sulciner ML, Serhan CN, Gilligan MM, Mudge DK, Chang J, Gartung A, Lehner KA, Bielenberg DR, Schmidt B, Dalli J, Greene ER, Gus-Brautbar Y, Piwowarski J, Mammoto T, Zurakowski D, Perretti M, Sukhatme VP, Kaipainen A, Kieran MW, Huang S, Panigrahy D (2018) Resolvins suppress tumor growth and enhance cancer therapy. J Exp Med 215:115–140
22. Gilligan MM, Gartung A, Sulciner ML, Norris PC, Sukhatme VP, Bielenberg DR, Huang S, Kieran MW, Serhan CN, Panigrahy D (2019) Aspirin-triggered proresolving mediators stimulate resolution in cancer. Proc Natl Acad Sci USA 16:6292–6297
23. Moore GY, Pidgeon GP (2017) Cross-talk between cancer cells and the tumour microenvironment: the role of the 5-lipoxygenase pathway. Int J Mol Sci 18:E236
24. Weigert A, Strack E, Snodgrass RG, Brune B (2018) mPGES-1 and ALOX5/-15 in tumor-associated macrophages. Cancer Metastasis Rev 37:317–334
25. Capra V, Rovati GE, Mangano P, Buccellati C, Murphy RC, Sala A (2015) Transcellular biosynthesis of eicosanoid lipid mediators. Biochim Biophys Acta 1851:377–382
26. Raasch M, Rennert K, Jahn T, Peters S, Henkel T, Huber O, Schulz I, Becker H, Lorkowski S, Funke H, Mosig A (2015) Microfluidically supported biochip design for culture of endothelial cell layers with improved perfusion conditions. Biofabrication 7:015013
27. Werz O, Gerstmeier J, Libreros S, De la Rosa X, Werner M, Norris PC, Chiang N, Serhan CN (2018) Human macrophages differentially produce specific resolvin or leukotriene signals that depend on bacterial pathogenicity. Nat Commun 9:59
28. Werner M, Jordan PM, Romp E, Czapka A, Rao Z, Kretzer C, Koeberle A, Garscha U, Pace S, Claesson HE, Serhan CN, Werz O, Gerstmeier J (2019) Targeting biosynthetic networks of the proinflammatory and proresolving lipid metabolome. FASEB J 33:6140–6153
29. Pace S, Pergola C, Dehm F, Rossi A, Gerstmeier J, Troisi F, Pein H, Schaible AM, Weinigel C, Rummler S, Northoff H, Laufer S, Maier TJ, Radmark O, Samuelsson B, Koeberle A, Sautebin L,

Werz O (2017) Androgen-mediated sex bias impairs efficiency of leukotriene biosynthesis inhibitors in males. J Clin Invest 127:3167–3176

30. Murray PJ, Allen JE, Biswas SK, Fisher EA, Gilroy DW, Goerdt S, Gordon S, Hamilton JA, Ivashkiv LB, Lawrence T, Locati M, Mantovani A, Martinez FO, Mege JL, Mosser DM, Natoli G, Saeij JP, Schultze JL, Shirey KA, Sica A, Suttles J, Udalova I, van Ginderachter JA, Vogel SN, Wynn TA (2014) Macrophage activation and polarization: nomenclature and experimental guidelines. Immunity 41:14–20

31. Li J, Diao B, Guo S, Huang X, Yang C, Feng Z, Yan W, Ning Q, Zheng L, Chen Y, Wu Y (2017) VSIG4 inhibits proinflammatory macrophage activation by reprogramming mitochondrial pyruvate metabolism. Nat Commun 8:1322

32. Dalli J, Serhan CN (2012) Specific lipid mediator signatures of human phagocytes: microparticles stimulate macrophage efferocytosis and pro-resolving mediators. Blood 120:e60–72

33. Araujo P, Belghit I, Aarsaether N, Espe M, Lucena E, Holen E (2019) The effect of omega-3 and omega-6 polyunsaturated fatty acids on the production of cyclooxygenase and lipoxygenase metabolites by human umbilical vein endothelial cells. Nutrients 11:E966

34. Mosca M, Polentarutti N, Mangano G, Apicella C, Doni A, Mancini F, De Bortoli M, Coletta I, Polenzani L, Santoni G, Sironi M, Vecchi A, Mantovani A (2007) Regulation of the microsomal prostaglandin E synthase-1 in polarized mononuclear phagocytes and its constitutive expression in neutrophils. J Leukoc Biol 82:320–326

35. Werz O, Steinhilber D (2005) Development of 5-lipoxygenase inhibitors—lessons from cellular enzyme regulation. Biochem Pharmacol 70:327–333

36. Radmark O, Werz O, Steinhilber D, Samuelsson B (2015) 5-Lipoxygenase, a key enzyme for leukotriene biosynthesis in health and disease. Biochim Biophys Acta 1851:331–339

37. Koeberle SC, Romir J, Fischer S, Koeberle A, Schattel V, Albrecht W, Grutter C, Werz O, Rauh D, Stehle T, Laufer SA (2011) Skepinone-L is a selective p38 mitogen-activated protein kinase inhibitor. Nat Chem Biol 8:141–143

38. Werz O, Burkert E, Samuelsson B, Radmark O, Steinhilber D (2002) Activation of 5-lipoxygenase by cell stress is calcium independent in human polymorphonuclear leukocytes. Blood 99:1044–1052

39. Werz O, Klemm J, Samuelsson B, Radmark O (2000) 5-lipoxygenase is phosphorylated by p38 kinase-dependent MAPKAP kinases. Proc Natl Acad Sci USA 97:5261–5266

40. Mazaleuskaya LL, Lawson JA, Li X, Grant G, Mesaros C, Grosser T, Blair IA, Ricciotti E, FitzGerald GA (2016) A broad-spectrum lipidomics screen of antiinflammatory drug combinations in human blood. JCI Insight 1:e87031

41. Mantovani A, Marchesi F, Malesci A, Laghi L, Allavena P (2017) Tumour-associated macrophages as treatment targets in oncology. Nat Rev Clin Oncol 14:399–416

42. Poczobutt JM, Gijon M, Amin J, Hanson D, Li H, Walker D, Weiser-Evans M, Lu X, Murphy RC, Nemenoff RA (2013) Eicosanoid profiling in an orthotopic model of lung cancer progression by mass spectrometry demonstrates selective production of leukotrienes by inflammatory cells of the microenvironment. PLoS ONE 8:e79633

43. Hong SH, Avis I, Vos MD, Martinez A, Treston AM, Mulshine JL (1999) Relationship of arachidonic acid metabolizing enzyme expression in epithelial cancer cell lines to the growth effect of selective biochemical inhibitors. Cancer Res 59:2223–2228

44. Luo M, Lee S, Brock TG (2003) Leukotriene synthesis by epithelial cells. Histol Histopathol 18:587–595

45. Lukic A, Wahlund CJE, Gomez C, Brodin D, Samuelsson B, Wheelock CE, Gabrielsson S, Radmark O (2019) Exosomes and cells from lung cancer pleural exudates transform LTC4 to LTD4, promoting cell migration and survival via CysLT1. Cancer Lett 444:1–8

46. Nosaka T, Baba T, Tanabe Y, Sasaki S, Nishimura T, Imamura Y, Yurino H, Hashimoto S, Arita M, Nakamoto Y, Mukaida N (2018) Alveolar macrophages drive hepatocellular carcinoma lung metastasis by generating leukotriene B4. J Immunol 200:1839–1852

47. Cheon EC, Khazaie K, Khan MW, Strouch MJ, Krantz SB, Phillips J, Blatner NR, Hix LM, Zhang M, Dennis KL, Salabat MR, Heiferman M, Grippo PJ, Munshi HG, Gounaris E, Bentrem DJ (2011) Mast cell 5-lipoxygenase activity promotes intestinal polyposis in APCDelta468 mice. Cancer Res 71:1627–1636

48. Wen Z, Liu H, Li M, Li B, Gao W, Shao Q, Fan B, Zhao F, Wang Q, Xie Q, Yang Y, Yu J, Qu X (2015) Increased metabolites of 5-lipoxygenase from hypoxic ovarian cancer cells promote tumor-associated macrophage infiltration. Oncogene 34:1241–1252

49. Poczobutt JM, Nguyen TT, Hanson D, Li H, Sippel TR, Weiser-Evans MC, Gijon M, Murphy RC, Nemenoff RA (2016) Deletion of 5-lipoxygenase in the tumor microenvironment promotes lung cancer progression and metastasis through regulating T cell recruitment. J Immunol 196:891–901

50. Ringleb J, Strack E, Angioni C, Geisslinger G, Steinhilber D, Weigert A, Brune B (2018) Apoptotic cancer cells suppress 5-lipoxygenase in tumor-associated macrophages. J Immunol 200:857–868

51. Werz O, Szellas D, Steinhilber D, Radmark O (2002) Arachidonic acid promotes phosphorylation of 5-lipoxygenase at Ser-271 by MAPK-activated protein kinase 2 (MK2). J Biol Chem 277:14793–14800

52. Werz O, Burkert E, Fischer L, Szellas D, Dishart D, Samuelsson B, Radmark O, Steinhilber D (2002) Extracellular signal-regulated kinases phosphorylate 5-lipoxygenase and stimulate 5-lipoxygenase product formation in leukocytes. FASEB J 16:1441–1443

53. Leslie CC (2015) Cytosolic phospholipase A(2): physiological function and role in disease. J Lipid Res 56:1386–1402

54. Gijon MA, Spencer DM, Siddiqi AR, Bonventre JV, Leslie CC (2000) Cytosolic phospholipase A2 is required for macrophage arachidonic acid release by agonists that do and do not mobilize calcium. Novel role of mitogen-activated protein kinase pathways in cytosolic phospholipase A2 regulation. J Biol Chem 275:20146–20156

55. Giannattasio G, Lai Y, Granata F, Mounier CM, Nallan L, Oslund R, Leslie CC, Marone G, Lambeau G, Gelb MH, Triggiani M (2009) Expression of phospholipases A2 in primary human lung macrophages: role of cytosolic phospholipase A2-alpha in arachidonic acid release and platelet activating factor synthesis. Biochim Biophys Acta 1791:92–102

56. Sulciner ML, Gartung A, Gilligan MM, Serhan CN, Panigrahy D (2018) Targeting lipid mediators in cancer biology. Cancer Metastasis Rev 37:557–572

57. Tian R, Zuo X, Jaoude J, Mao F, Colby J, Shureiqi I (2017) ALOX15 as a suppressor of inflammation and cancer: lost in the link. Prostaglandin Other Lipid Mediat 132:77–83

58. Daurkin I, Eruslanov E, Stoffs T, Perrin GQ, Algood C, Gilbert SM, Rosser CJ, Su LM, Vieweg J, Kusmartsev S (2011) Tumor-associated macrophages mediate immunosuppression in the renal cancer microenvironment by activating the 15-lipoxygenase-2 pathway. Cancer Res 71:6400–6409

59. Hashemi Goradel N, Najafi M, Salehi E, Farhood B, Mortezaee K (2019) Cyclooxygenase-2 in cancer: a review. J Cell Physiol 234:5683–5699

60. Muller-Decker K (2011) Cyclooxygenase-dependent signaling is causally linked to non-melanoma skin carcinogenesis: pharmacological, genetic, and clinical evidence. Cancer Metastasis Rev 30:343–361

61. Xia D, Wang D, Kim SH, Katoh H, DuBois RN (2012) Prostaglandin E2 promotes intestinal tumor growth via DNA methylation. Nat Med 18:224–226

62. Hanayama R, Tanaka M, Miwa K, Shinohara A, Iwamatsu A, Nagata S (2002) Identification of a factor that links apoptotic cells to phagocytes. Nature 417:182–187

63. Soki FN, Koh AJ, Jones JD, Kim YW, Dai J, Keller ET, Pienta KJ, Atabai K, Roca H, McCauley LK (2014) Polarization of prostate cancer-associated macrophages is induced by milk fat globule-EGF factor 8 (MFG-E8)-mediated efferocytosis. J Biol Chem 289:24560–24572